

Raman tweezers provide the fingerprint of cells supporting the late stages of KSHV reactivation

Ossie F. Dyson^{a, #}, Patrick W. Ford^{a, #}, De Chen^b, Yong-Qing Li^b, Shaw M. Akula^{a, *}

^a Department of Microbiology & Immunology, Brody School of Medicine at East Carolina University, Greenville, NC, USA

^b Department of Physics, East Carolina University, Greenville, NC, USA

Received: June 5, 2008; Accepted: August 12, 2008

Abstract

Kaposi's sarcoma-associated herpesvirus (KSHV) has both latent and lytic phases of replication. The molecular switch that triggers a reactivation is still unclear. Cells from the S phase of the cell cycle provide apt conditions for an active reactivation. In order to specifically delineate the Raman spectra of cells supporting KSHV reactivation, we followed a novel approach where cells were sorted based on the state of infection (latent *versus* lytic) by a flow cytometer and then analysed by the Raman tweezers. The Raman bands at 785, 813, 830, 1095 and 1128 cm^{-1} are specifically altered in cells supporting KSHV reactivation. These five peaks make up the Raman fingerprint of cells supporting KSHV reactivation. The physiological relevance of the changes in these peaks with respect to KSHV reactivation is discussed in the following report.

Keywords: KSHV • latency • S phase • Raman tweezers • reactivation

Introduction

Kaposi's sarcoma-associated herpesvirus (KSHV), also known as human herpesvirus-8 was first described in 1994 [1]. KSHV is etiologically associated with all forms of Kaposi sarcoma, primary effusion lymphoma (PEL) and multi-centric Castlemann disease [2, 3]. Apart from the inflammatory cytokines/growth factors, lytic KSHV infection plays an instrumental role in the progression of Kaposi sarcoma lesions [4–6]. Successful KSHV infection is characterized by both virus entry and the ability of the virus to establish latency. The lytic infection is also critical for the spread of KSHV to different organs.

KSHV infects a variety of target cells that includes human B cells, macrophages, keratinocytes, endothelial cells and epithelial cells [7–11]. However, all of these infections are either abortive and/or latent, which are characterized by the presence of circular latent viral DNA and by the expression of KSHV latency-associated nuclear antigen (LANA) encoded by ORF73 [12]. Generally, a lytic cycle of KSHV infection can be induced in cells harbouring latent

KSHV by treatment with phorbol-12-myristate-13-acetate (TPA) or sodium butyrate [13].

The concept of latency is not new to the field of herpesvirology. Herpes simplex virus (an α -herpesvirus), human cytomegalovirus (a β -herpesvirus) and KSHV (a γ -herpesvirus) are examples of viruses from the three different herpesvirus families that cause latent infection of cells [14]. There are several other viruses that cause latent infections of target cells. Some of the other examples are hepatitis B virus, Epstein–Barr virus and adenovirus [15, 16]. Any form of stress, treatment with immunosuppressant drugs or immune suppression has been demonstrated to reactivate herpesviruses from latency [17–19]. However, the exact mechanism for the reactivation of herpesvirus latency is still eluding. Understanding latency better will have an immediate impact on the economy as it will help us develop good antiviral/vaccine strategies for the benefit of the mankind. For all along, relying purely on only the conventional biochemical and molecular biology approaches have not been fruitful to delineate virus latency. Knowledge on reactivation of latent virus infections in general remains limited.

Raman tweezers involve confocal microscopy, which incorporates the use of both laser (optical) tweezers and Raman spectroscopy (LTRS) [20]. The optical tweezers part of the LTRS system uses a focused near infrared (NIR) beam at 785 nm to immobilize a cell, whereas the Raman spectroscopy part of this

Q1 [#] These authors contributed equally.

*Correspondence to: Shaw M. AKULA,
Department of Microbiology & Immunology, Brody School of Medicine,
East Carolina University, Greenville, NC 27834, USA.
Tel.: +(252)744-2702
Fax: +(252) 744-3104
E-mail: akulas@ecu.edu

1 system uses the same NIR beam to generate the vibrational
2 spectra of the immobilized cell. The basic steps to obtain the
3 vibrational spectra of living cells using Raman tweezers include
4 the following: (i) The cells will be illuminated with the NIR beam;
5 (ii) The molecules in the cells at a particular state will scatter the
6 incident light in a specific and unique pattern and (iii) The scatter-
7 ed light will be collected and analysed using a system com-
8 prising of lenses and a charge-coupled device (CCD) camera to
9 provide the Raman spectra (detailed in the review by Lambert
10 *et al.* [21]). We made the assumption that the changes in the cel-
11 lular environment during different stages of virus replication will
12 be reflected in the Raman spectra. Furthermore, if these spectral
13 changes are specific enough for a particular stage of replication,
14 they can, in principle, be used as a bio-marker of the replication
15 stage. Hence, in this study we attempted to decipher the crucial
16 fingerprints of cells capable of supporting KSHV reactivation by
17 a combination of biochemical assays, molecular biology, and
18 Raman tweezers.

19 In order to analyse KSHV reactivation, we used PEL cells
20 (BCBL-1 and BCP-1 cells; both of which are KSHV infected human
21 B cells) in this study. PEL cells turned out to be a blessing in dis-
22 guise as they naturally harbour KSHV in a latent form and that a
23 lytic infection may be induced conditionally by treating them with
24 TPA [22]. Herein, we provide for the first time the Raman finger-
25 print of cells supporting KSHV reactivation. There are several
26 advantages of using Raman tweezers to analyse biological speci-
27 mens [21] of which the most important one with respect to
28 the present study is the fact that it allows for the analysis of the
29 sample without physically touching it, thereby leaving the cell in a
30 less disturbed and more natural state [23]. Taken together, such
31 an approach may well be exploited to understand a variety of viral
32 infections with special emphasis to replication stages so that it
33 may serve as a diagnostic tool in the near future.

34 35 36 37 38 39 40 41 42 43 44 45 46 47 48 49 50 51 52 53 54 55

Materials and methods

Cells

BCBL-1 and BCP-1 cells were used in this study. These cells were grown in phenol red-free RPMI medium (Invitrogen, Carlsbad, CA, USA) containing 10% charcoal stripped foetal bovine serum (FBS) (Atlanta Biologicals, Inc., Lawrenceville, GA, USA), L-glutamine and antibiotics [24].

Transfection of cells with p16INK4A plasmid

Target cells were grown in six-well plates to a concentration of 1×10^6 cells/ml. These cells were untransfected, transfected with the empty vector (pCND3.1) or transfected with p16INK4A/pCND3.1 (encoding the full length p16INK4A gene) [25] with Gene Jammer (Stratagene, La Jolla, CA, USA) as per the manufacturer's recommendations. After 48 hrs transfection, these cells (transiently transfected) were used in other experiments to analyse the role of p16INK4A in regulating KSHV reactivation.

Quantitative real-time PCR (qRT-PCR)

Total RNA was isolated using a Nucleospin RNA II kit (Clontech, Palo Alto, CA, USA) as per manufacturer's recommendations. The cDNA was synthesized from the total RNA (500 ng) using the First-Strand cDNA Synthesis System (Invitrogen). The qRT-PCR was performed using the synthesized cDNA in single wells of a 96-well plate (BioRad, Hercules, CA, USA) in a 25- μ l reaction volume to analyse the expression of TK1 and β -actin transcripts as per earlier protocols using specific primers [26, 27]. The thermocycling program consisted of 95°C for 3 min., followed by 40 cycles of 95°C for 15 sec. and 60°C for 45 sec. The specificity and purity of the amplification reaction was determined by performing a melting curve analysis.

Western blotting

All the buffers used in this project were made with water that was endotoxin and pyrogen free. Equal amounts (25 μ g) of protein were used in Western blotting experiments [26]. The Western blots were routinely probed first with mouse anti-p16INK4A antibody (Clone ZJ11; Chemicon International, Temecula, CA, USA). These blots were then 'stripped' for reprobing with mouse anti-actin antibodies (Clone AC-74; Sigma, St. Louis, MO, USA) as per standard protocols [28].

Immunofluorescence assay (IFA)

Target cells were washed twice in phosphate-buffered saline (PBS), spotted on glass slides, air-dried and then fixed in ice-cold acetone for 10 min. The fixed cells were washed in PBS and stained sequentially with rabbit anti-gB antibodies [29] and goat anti-rabbit fluorescein isothiocyanate (FITC)-labelled secondary antibody (KPL, Gaithersburg, MD, USA) for 30 min. at 37°C. Stained cells were washed with PBS and were further incubated for 20 min. at room temperature with 5 mM SYTO Red (a nuclear stain; Invitrogen) before being washed again and examined under a fluorescent microscope (Nikon Eclipse E600) with appropriate filters. In another set of experiments, acetone fixed target cells were stained simultaneously for the expression of KSHV gB and LANA with rabbit anti-gB antibodies and monoclonal antibodies to LANA (ABI, Columbia, MD, USA), respectively. These cells were further incubated for 30 min. with TRITC conjugated goat anti-rabbit antibodies and FITC conjugated goat anti-mouse antibodies as per procedures outlined above before being analysed under a fluorescent microscope. The mean number of positive cells counted over five random fields was used for comparison and analysis. Arrowheads indicate cells that are positive for gB expression.

Synchronizing cells in different phases of cell cycle

We synchronized BCBL-1 and BCP-1 cells in G0/1 and S phase of cell cycle as per standard protocols [27, 30]. Briefly, cells were synchronized at G0/1 by 24 hrs of incubation in serum-free RPMI 1640 medium supplemented with antibiotics and 2 mM glutamine. Cells were synchronized at S phase of cell cycle by culturing the above (those synchronized in G0/1 phase) cells in RPMI 1640 medium supplemented with 10% FBS, antibiotics and 2 mM glutamine for 16 hrs.

Flow cytometry

Flow cytometer was used to analyse cells in different stages of cell cycle. A 10 $\mu\text{g/ml}$ concentration of Hoechst dye 33342 (Sigma) was added to the target cell suspension and incubated further at 37°C for 45 min. These cells were analysed by FACScan flow cytometer (Becton Dickinson, San Jose, CA, USA) to discriminate cells in different stages of cell cycle as per earlier protocols [28]. For another experiment, cells in S phase were treated with 20 ng/ml of TPA. After 36 hrs TPA treatment, these cells were washed twice in cold PBS and stained with rabbit anti-gB antibodies for 30 min. on ice. The cells were washed thrice in cold PBS and further incubated with a pre-determined concentration of anti-rabbit antibodies conjugated to FITC (Sigma). After 30 min. of incubation, these cells were washed as before and sorted for cells expressing gB on their surface using a FACScan flow cytometer (Becton Dickinson) as per standard lab protocols [28]. These gB positive sorted cells were washed twice in growth medium and further incubated for another 4 hrs at 37°C before being analysed by Raman tweezers.

Trypan blue test

Target cell survival was measured by staining cells with trypan blue solution (Sigma) diluted to a final concentration of 0.04% (w/v). Stained cells were visualized using bright field microscopy at 100 \times magnification. The number of viable (unstained) and non-viable (blue stained) cells were recorded as per standard procedure [31].

Analysing cells by Raman tweezers

A detailed description of the Raman tweezers is provided in our earlier study [32]. Raman spectra for the different target cells were acquired using a spectrograph (Triax 320, Jobin Yvon Ltd., Edison, NJ, USA) equipped with a liquid nitrogen cooled CCD detector. The Raman signal was collected in the spectral interval from 400 to 2100 cm^{-1} with a resolution of 6 cm^{-1} . Spectral acquisition for each cell was performed with a collection time of 60 sec., 20 mW at 780 nm. All the cells analysed by this procedure were suspended in phenol red-free RPMI medium. Each individual cell was held in the laser beam and elevated from the cover slide about 10 μm to reduce the Brownian motion of the cell during the Raman acquisition and to reduce the fluorescence background from the glass cover slide. The Raman spectra of twenty cells were acquired for each cell type. Such single blinded studies were performed thrice on three different days. Fresh samples were used after acquisition of data for 10 cells. The background was recorded with the same acquisition conditions without trapping cells. Following spectral acquisition, the background signal originating from the cover slide and the surrounding medium was subtracted from all the spectra. The subtracted spectra were calibrated with the spectral response function of the Raman system.

Results

Cell cycle is a determining factor for KSHV reactivation

KSHV reactivation is still an enigma. Recent studies demonstrated that the cells in S phase of cell cycle provide KSHV with the apt

environment for a productive lytic cycle of infection or reactivation [28, 30]. The above studies used cells sorted by flow cytometry [28] and serum starvation method [30] to arrive at the same conclusion. In this study, we go a step further in that we analysed the effect of endogenously overexpressing p16INK4A and analysing its effect of KSHV reactivation. p16INK4A promotes G0/1 phase cell cycle arrest that is primarily dependent on a functional Rb protein [33]. KSHV infected BCBL-1 cells do not express p16INK4A [34]. BCBL-1 cells transfected with p16INK4A/pCDNA3.1 expressed elevated levels of p16INK4A when compared to cells transfected with empty vector (pCDNA3.1) (Fig. 1A). Untransfected cells did not express significant amounts of p16INK4A as observed by Western blotting experiments (Fig. 1A). Cells transfected with p16INK4A/pCDNA3.1 resulted in an increase in the number of cells in G0/1 phase when compared to cells that were untransfected (Fig. 1B and C). Transfection of cells with the empty vector did not significantly alter the cell cycle progression (Fig. 1C). Next, we treated the above-transfected cells with 20 ng/ml of TPA for 34 hrs and analysed for a possible reactivation of KSHV infection by monitoring gB (late lytic protein) by IFA. KSHV genome is maintained predominantly in a latent phase in BCBL-1 cells. Only 1–3% of cells spontaneously support lytic infection [35]. Expression of gB protein is an indicator of KSHV reactivation in BCBL-1 cells. Treatment of untransfected cells with TPA induced a significantly higher number of cells that supported a lytic infection as observed by the expression of gB (Fig. 1D). Identical results were observed in cells that were transfected with empty vector and TPA induced (Fig. 1D). However, TPA treatment of cells transfected with p16INK4A/pCDNA3.1 significantly lowered the expression of gB (Fig. 1D and E). Interestingly, cells expressing p16INK4A stained positive for LANA but negative for gB (data not shown). Taken together, our results clearly indicate that the cells in G0/1 phase are less permissive to lytic infection when compared to those in S phase. These results corroborate with the earlier findings that cell cycle plays a crucial role in determining KSHV reactivation [28, 30]. Target cells in S phase support reactivation to a significantly greater level when compared to those in G0/1 phase.

Analysis of BCBL-1 cells from different phases of cell cycle by Raman spectroscopy

A population of cells can be broadly divided into three groups based on cell cycle as G0/1, S and G2/M phases. BCBL-1 cells harbour KSHV predominantly in a latent form. A lytic cycle of KSHV infection is supported primarily by BCBL-1 cells in S phase. As a first step towards delineating KSHV reactivation, we planned to obtain the Raman spectra of BCBL-1 cells in S phase that are capable of supporting a lytic infection. Towards this, cells were sorted in different phases of cell cycle by the conventional approach of serum starving [36]. Briefly, the cells were arrested in G0/1 phase of cell cycle by serum starving them for 24 hrs. These cells were further incubated with 10% FBS at 37°C. After 16 hrs incubation, the cells were found to be predominantly in S phase of

1
2
3
4
5
6
7
8
9
10
11
12
13
14
15
16
17
18
19
20
21
22
23
24
25
26
27
28
29
30
31
32
33
34
35
36
37
38
39
40
41
42
43
44
45
46
47
48
49
50
51
52
53
54
55

Q8

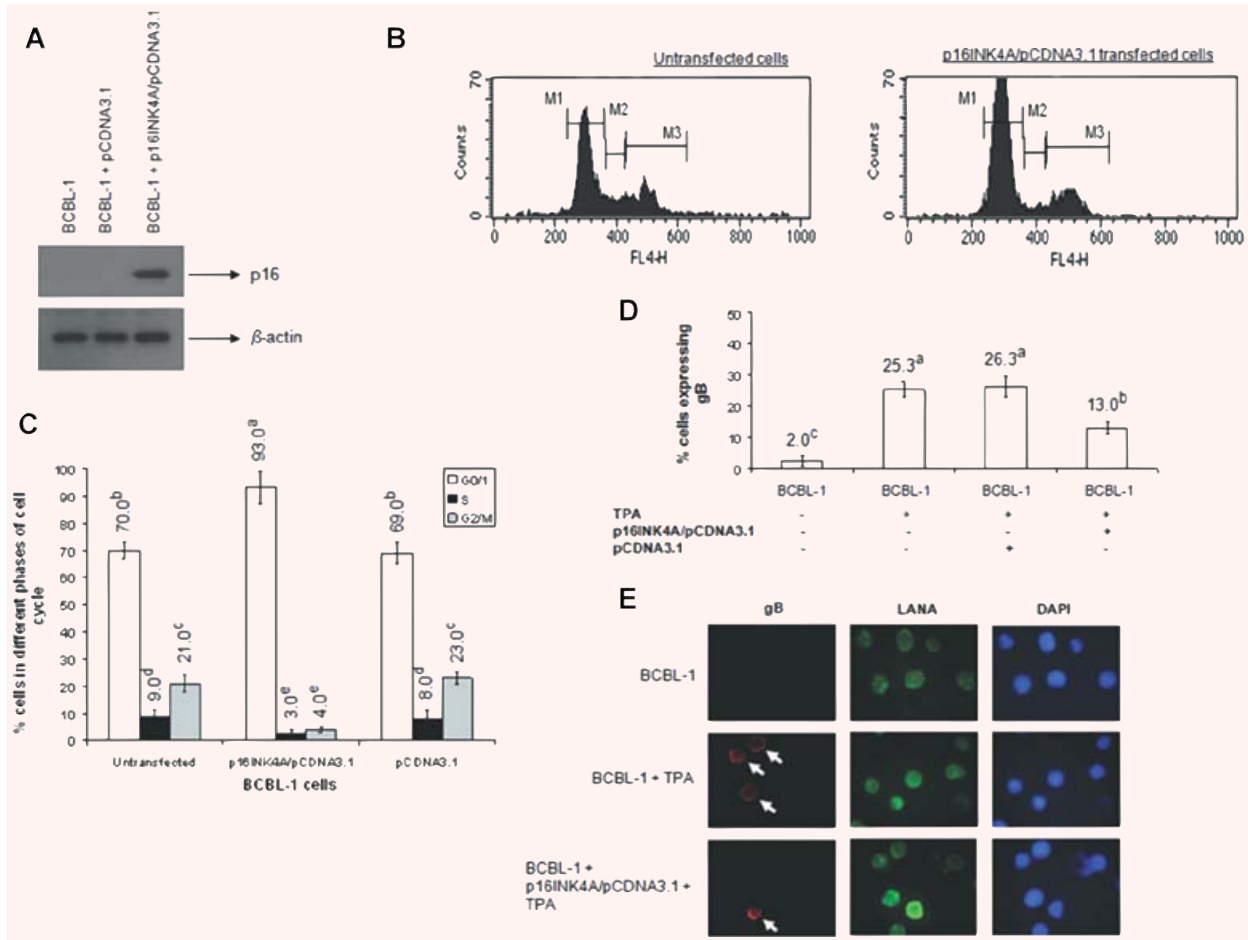


Fig. 1 Ectopic expression of p16INK4A induces cell cycle arrest in G0/1 phase resulting in a decreased response to TPA-induced reactivation. **(A)** BCBL-1 cells were untransfected, transfected with empty vector (pCDNA3.1), or p16INK4A/pCDNA3.1. Western blot analysis of p16INK4A and β -actin expression in the above cells was performed at 48 hrs after transfection. The bands were scanned and the band intensities were assessed using the ImageQuaNT software program (Molecular Dynamics). **(B)** Flow cytometer was used to analyse cell cycle in target cells. Representative histograms depicting cell cycle in untransfected and p16INK4A/pCDNA3.1 transfected BCBL-1 cells stained with Hoechst dye 33342 is shown. **(C)** The percentage number of cells in different phases of cell cycle is provided based on the results from three different trials. Data presented represent the average \pm S.D. of three experiments. Average values on the columns with different superscripts are statistically significant ($P < 0.05$) by least significant difference (LSD). **(D)** Immunofluorescence assay (IFA) was performed to analyse the expression of gB in the above cells. The percentage cells expressing gB under different conditions is provided. Data presented represent the average \pm S.D. of three experiments. Average values on the columns with different superscripts are statistically significant ($P < 0.05$) by LSD. Representative images of IFA experimentation is provided for reference **(E)**. Magnification: 100 \times .

cell cycle [30, 37]. This was also confirmed by monitoring the expression of thymidine kinase 1 (TK1) gene by qRT-PCR. TK1, a cell cycle-dependent enzyme involved in the synthesis of DNA, is histological marker for cell proliferation [38]. TK1 gene expression is highly elevated in cells that enter S phase of cell cycle (actively dividing) whereas it is limited or almost absent in G0/1 phase, quiescent cells [28, 39, 40]. As expected, TK1 gene expression was sixfold higher in BCBL-1 cells obtained 16 hrs after FBS treatment of serum starved cells (S phase of cell cycle) when compared to

those obtained 24 hrs after serum starvation (G0/1 phase) (Fig. 2A). No detectable signal was observed with reactions performed in the absence of template (data not shown), demonstrating the specificity of the qRT-PCR conducted.

Raman spectra were obtained for cells from three different groups: (i) cells in G0/1 phase, (ii) cells in S phase and (iii) cells from S phase that were TPA induced for 48 hrs. The basis for selecting these three groups is the inherent variation in the cellular environment among the three groups with respect to KSHV

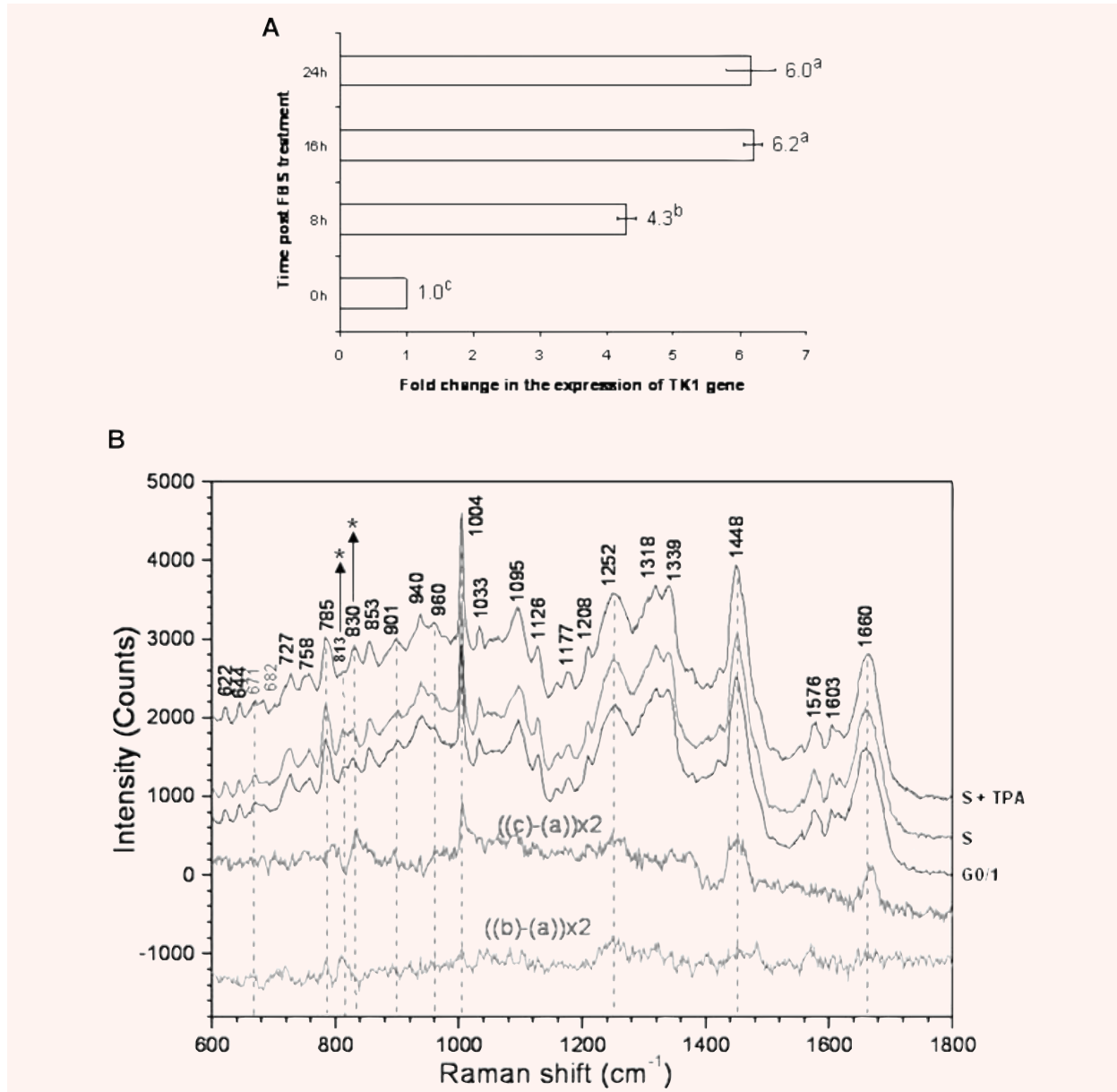


Fig. 2 (A) BCBL-1 cells in S phase express elevated levels of TK1. BCBL-1 cells were serum starved for 24 hrs. These cells were incubated in RPMI containing 10% foetal bovine serum (FBS). The cells were collected at 0, 8, 16 and 24 hrs after FBS addition, lysed, RNA extracted and qRT-PCR performed as per standard protocols. The fold increase in the expression of TK1 gene expression is represented in histogram and was calculated based on the standard graph generated by qRT-PCR of a known concentration of the TK1 gene. Expression of TK1 gene at 0 hrs was considered as onefold. The lowest limit of detection in the standard samples was 6 to 60 copies for the TK1 gene. The data presented in the histogram was from three independent experiments. Average values on columns with different superscripts are statistically significant ($P < 0.05$) by least significant difference (LSD). **(B)** Raman spectra of BCBL-1 cells from different stages of cell cycle. Average Raman spectra of individual BCBL-1 cells from G0/1, S, and S phase induced with TPA in the fingerprint range from 600 to 1800 cm⁻¹ is depicted. Raman bands that occur between BCBL-1 cells obtained from G0/1 (a), S (b), and S phase cells that were induced with TPA (c) is shown. Each spectrum was obtained by averaging the spectra of 20 individual cells. **(C)** Spectral changes in 785, 813, 830 and 1660 cm⁻¹ bands are shown. The spectra are an average of data from 20 cells. Average values on columns with different superscripts are statistically significant ($P < 0.05$) by LSD.

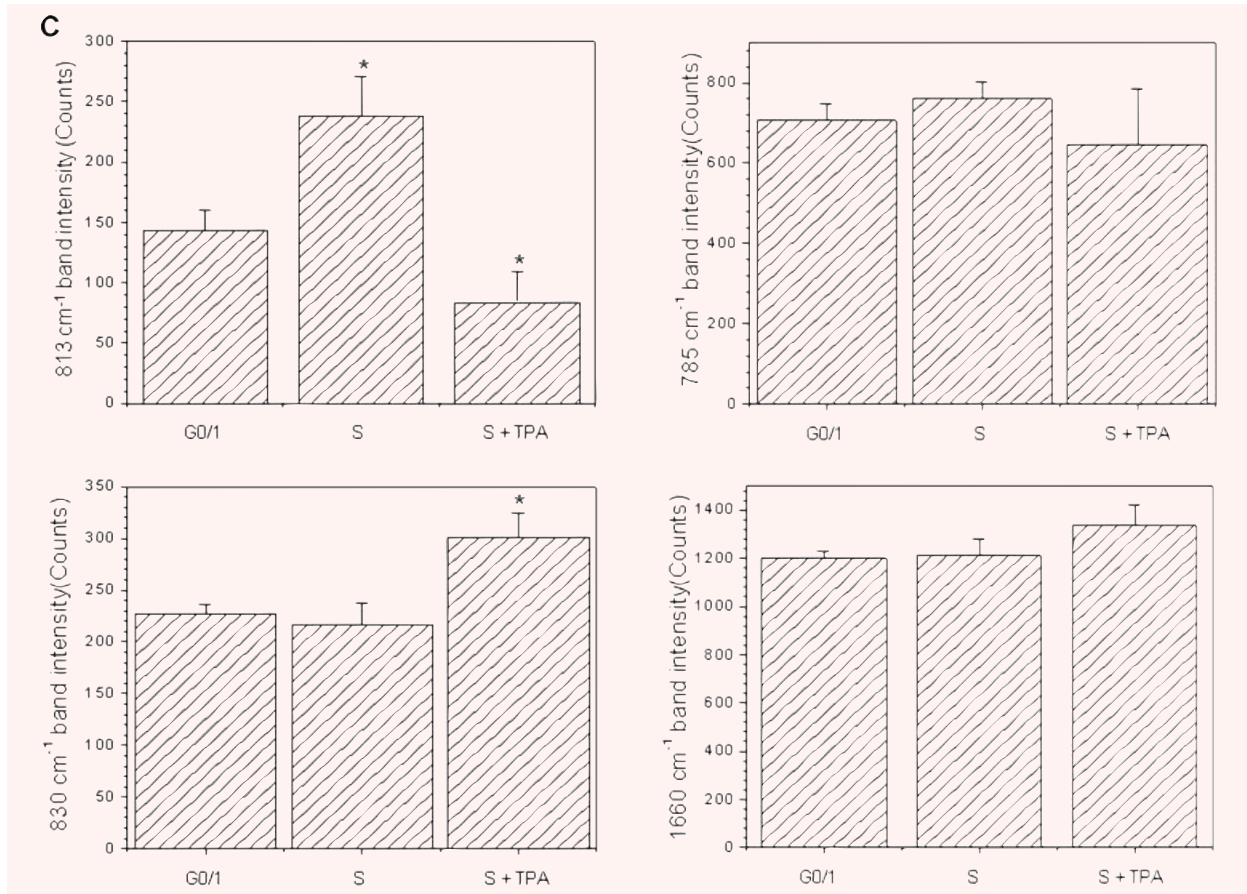


Fig. 2 Continued.

reactivation. The experimental set up for the Raman tweezers is described in the methods section. Each of these cells was trapped optically and analysed using Raman tweezers. The cells have a rounded morphology with an average diameter of 8–12 μm . For each cell type, the Raman acquisition was done only for the nuclei portion of the cells with the confocal LTRS system. The Raman spectrum of BCBL-1 cells under physiological conditions was recorded at 22°C (Fig. 2B). Among the other subtle differences, the intensities of the Raman bands at 813 and 830 cm^{-1} were significantly altered in the nucleus of KSHV infected cells from S phase and TPA-induced cells from S phase when compared to cells from G0/1 phase (Fig. 2B and C). The intensities of the Raman bands at 813 cm^{-1} were significantly greater in cells from S phase when compared to those in cells from G0/1 and TPA-induced cells from S phase (Fig. 2C). The 813 cm^{-1} band intensity was significantly lower in TPA-induced cells from S phase when compared to cells from G0/1 and S phase (Fig. 2C). On the same note, the intensity of band at 830 cm^{-1} was significantly greater in TPA-induced cells from S phase when compared to cells from G0/1 and S phase (Fig. 2C). The Raman spectra for S phase cells

treated with DMSO (the vehicle for TPA) was comparable to the one obtained for the cells from S phase (data not shown). Interestingly, the band intensities of the peaks at 785 and 1660 cm^{-1} between the three groups of cells remained comparable demonstrating the specificity of the Raman signals.

TPA treatment of cells results in an induction of a lytic infection in BCBL-1 cells. By 48 hrs after TPA induction, some cells start to show signs of death. In order to confirm that cells analysed by Raman tweezers were very much viable and not dead, we did two things as follows: (i) analysed percentage dead cells by trypan blue test and (ii) obtained Raman spectra of dead cells. Under our laboratory conditions, greater than 95% of cells were found to be viable in G0/1 and S phase (Fig. 3A). However, we determined $13 \pm 4\%$ of cells to be dead in TPA-induced cells from S phase (Fig. 3A). Under a bright field microscope, dead cells appear to have lost membrane integrity. We acquired the Raman spectra for such dead cells and found one unique peak that was significantly greater in them when compared to the viable cells in G0/1, S and TPA-induced cells from S phase (Fig. 3B). This was Raman band at 1050 cm^{-1} (Fig. 3B). Interestingly, this band was not observed

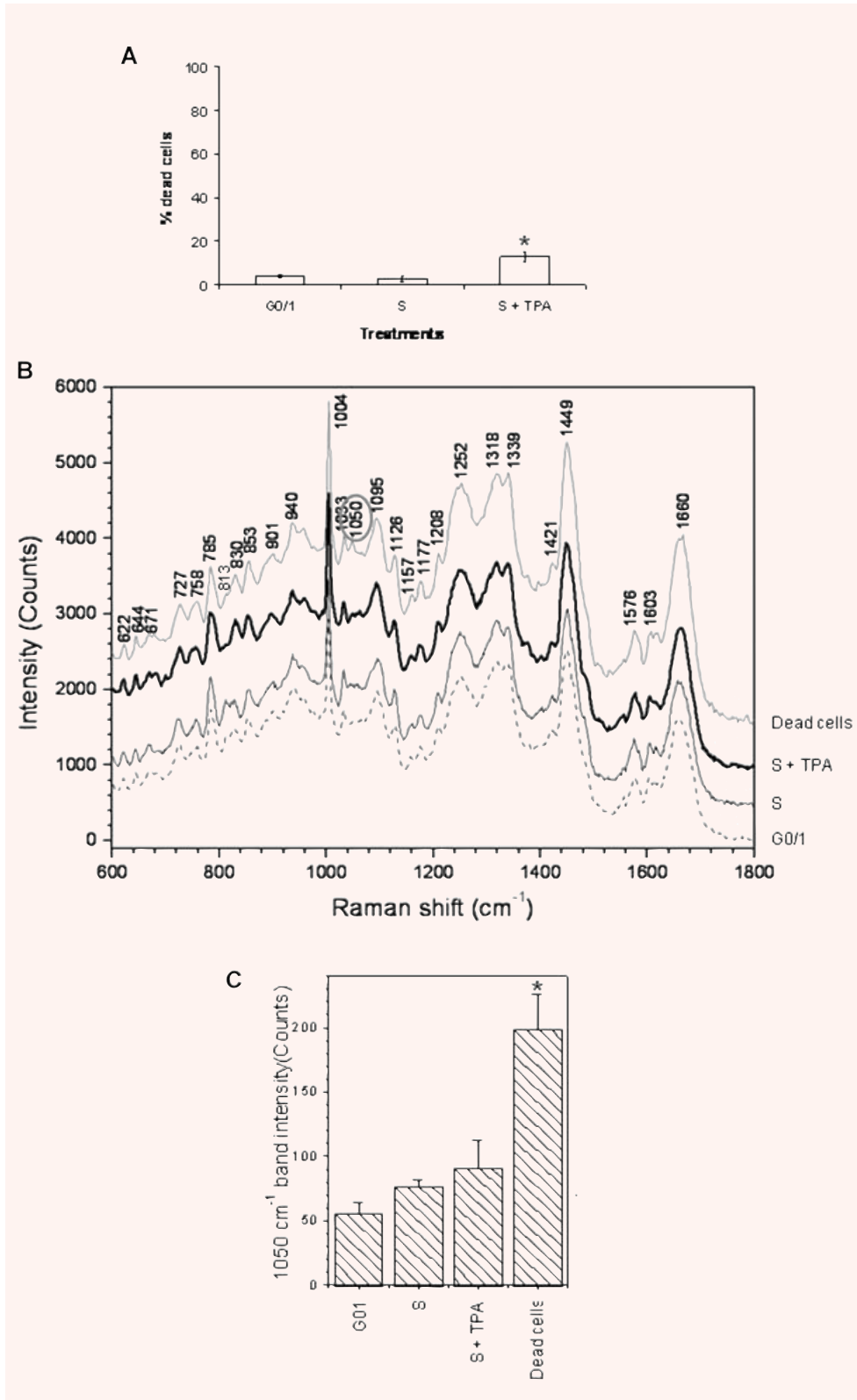


Fig. 3 Dead BCBL-1 cells have a distinct Raman band at 1050 cm^{-1} . **(A)** Data from trypan blue test to monitor percentage dead cells are shown. Data presented represent the average \pm S.D. of three experiments. The column with an asterisk mark indicates the value to be statistically significant ($P < 0.05$) by least significant difference (LSD). **(B)** Comparing Raman spectra of dead cells with the cells obtained from G0/1, S and TPA-induced S phase cells. Each spectrum was obtained by averaging the spectra of 20 individual cells. The Raman band at 1050 cm^{-1} is circled. **(C)** Spectral changes in 1050 cm^{-1} Raman band that occur between BCBL-1 cells obtained from G0/1, S, S phase cells that were induced with TPA, and dead cells is shown. The spectra are an average of data from 20 cells. The column with an asterisk mark indicates the value to be statistically significant ($P < 0.05$) by LSD.

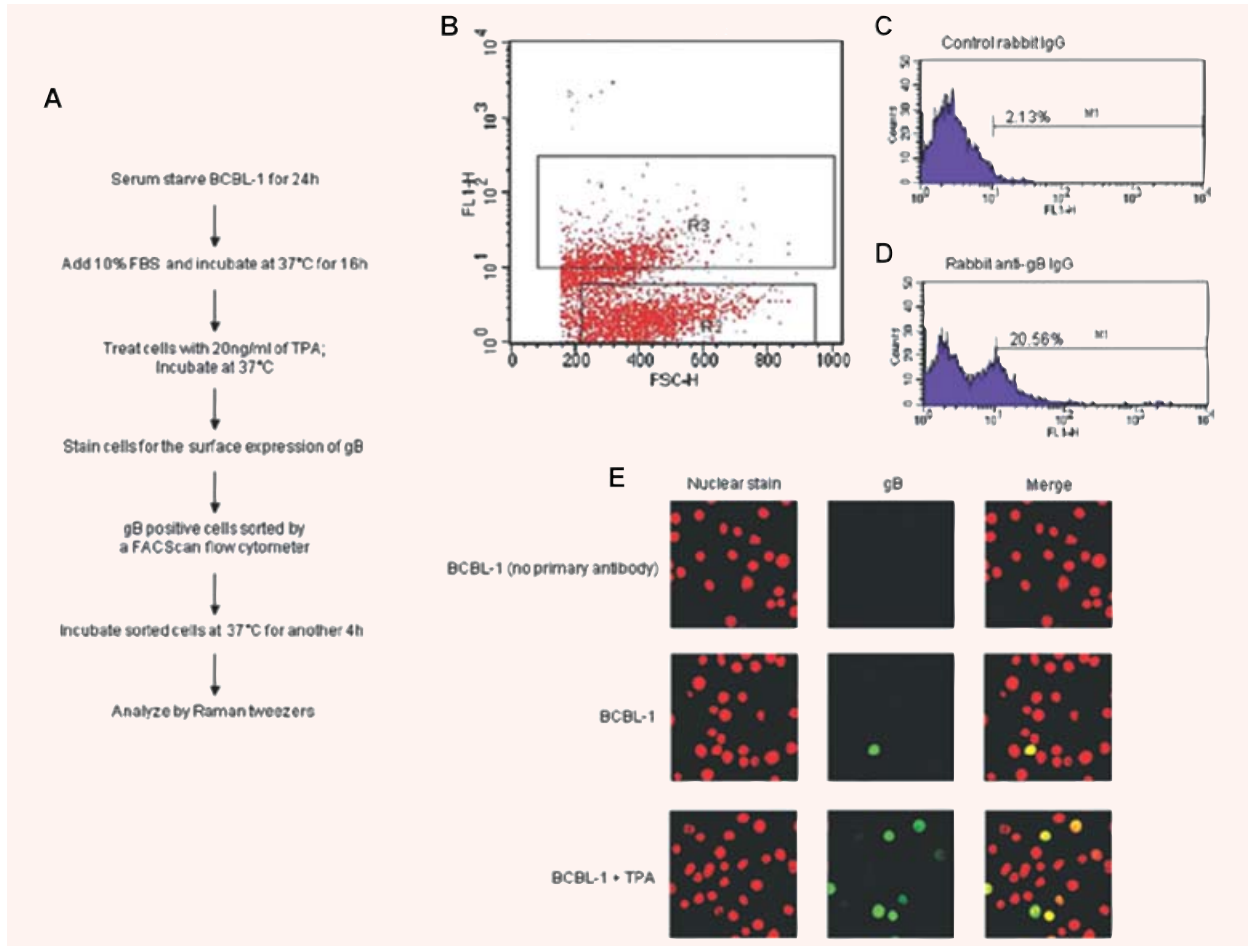


Fig. 4 Flow cytometer was used to sort cells that were actively supporting Kaposi's sarcoma-associated herpesvirus (KSHV) reactivation (A) Schematic line drawing showing the experimental protocol involved in assessing the fingerprint of BCBL-1 cells supporting KSHV reactivation. Cells in S phase were TPA treated for 36 hrs. These cells were stained for the surface expression of gB and analysed in a FACScan flow cytometer. (B) A representative forward- and side-scatter plot of these stained cells is provided. (C, D) Cells in R3 were sorted to obtain cells that were negative and positive for surface gB expression. (E) These sorted cells were incubated sequentially with rabbit polyclonal antibodies to gB and FITC-anti-rabbit antibodies. Finally, the stained cells were further incubated for 20 min. on ice with 5 mM SYTO Red (a nuclear stain; Invitrogen) and examined under a fluorescent microscope using respective filters. Magnification: 62 \times .

at the same intensity in cells from G0/1, S and TPA-induced cells from S phase (Fig. 3C). These results confirm the authenticity of our Raman bands for cells from G0/1, S and TPA-induced cells from S phase. Taken together, Raman tweezers successfully identified the crucial fingerprints of cells that have the propensity to support a lytic infection (cells from S phase).

Analysis of PEL cells specifically supporting KSHV reactivation by Raman tweezers

TPA treatment of cells induces KSHV lytic infection. However, the analysis of TPA-induced cells from S phase does not quite provide

the Raman bands that were specific to reactivation. This is partly because of the fact that TPA treatment of cells only induces reactivation in about 20–25% of the cells [35]. Hence, we attempted to obtain Raman spectra of flow cytometry sorted cells that were specifically undergoing reactivation. To authenticate our results, we used two different KSHV infected PEL cells in the following studies: BCBL-1 and BCP-1 cells [22].

The goal was achieved by analysing the flow cytometry sorted cells that were specifically undergoing reactivation by Raman tweezers as per protocols outlined in the schematic line drawing (Fig. 4A). The key was to sort cells expressing gB, an envelope-associated protein termed as a 'late protein', which is a classic indicator of a lytic infection [35]. Forward- and side-scatter plot

1 was used to gate the population of BCBL-1 (Fig. 4B) and BCP-1
 2 cells (data not shown) for sorting. We observed 20–25% of TPA-
 3 induced cells from S phase to express gB in BCBL-1 cells (Fig. 4C
 4 and D). Identical results were observed in TPA-induced BCP-1
 5 cells (data not shown). These results were further confirmed by
 6 IFA using rabbit anti-gB antibodies (Fig. 4E). The results from IFA
 7 Q9 studies corroborate the findings from FACs analysis.

8 Cells from S phase that were TPA-induced were screened in a
 9 flow cytometer, sorted based on the expression of gB and were
 10 analysed by Raman tweezers. Cells that were gB positive support-
 11 ed a KSHV lytic infection (reactivation), whereas cells that were gB
 12 negative supported a latent infection. All the cells analysed by
 13 Raman tweezers were live and not dead. This is also apparent by
 14 the absence of a strong Raman band at 1050 cm^{-1} (Fig. 5A and B).
 15 PEL cells supporting KSHV reactivation had weak and strong
 16 bands at 813 and 830 cm^{-1} , respectively (Fig. 5A and B). In addi-
 17 tion, there were three other peaks that were unique to cells sup-
 18 porting KSHV reactivation when compared to cells supporting a
 19 latent infection. PEL cells supporting virus reactivation had weak
 20 bands at 785 and 1095 cm^{-1} ; and a stronger band at 1128 cm^{-1}
 21 when compared to cells supporting a latent infection (Fig. 5A
 22 and B). Taken together, for the first time unique fingerprints of
 23 cells supporting KSHV reactivation has been delineated.

24 Discussion

25 There are several viruses that produce latent infection in target
 26 cells. These viruses have a specific phase during their replication
 27 cycle when a latent infection is terminated. Termination of latency
 28 leads to a lytic replication phase. As of this date, the exact mech-
 29 anism behind this switch from latent to lytic infection is still
 30 elusive. Herein, we have attempted to use a combination of bio-
 31 chemical assays, molecular biology tools and Raman tweezers to
 32 decipher the crucial signature of cells supporting virus reactiva-
 33 tion; and in the process, we have used KSHV as a model to analyse
 34 this goal. Raman spectroscopy has been previously used to
 35 understand several aspects of biology such as different stages of
 36 virus infection, biology of cancers and so on [32, 41–43].

37 TPA treatment of PEL cells transfected with p16INK4A/
 38 pCDNA3.1 did not significantly enhance lytic infection when com-
 39 pared to the untransfected cells (Fig. 1). The results from these
 40 transfection experiments supported the fact that the cells from S
 41 phase provide the optimal conditions for KSHV reactivation. These
 42 results support earlier findings by others and us [28, 30]. Hence,
 43 we acquired Raman specific bands for cells in G0/1, S and S phase
 44 cells treated with TPA. The spectra of all the cell types used in this
 45 study share many similar peaks that can be assigned to cellular
 46 constituents: nucleic acids (DNA/RNA), proteins, lipids and carbo-
 47 hydrates. The two major peaks that were found to be significantly
 48 altered between cells from G0/1, S, and cells from S phase that
 49 were TPA treated were at 813 and 830 cm^{-1} (Fig. 2B and C). The
 50 Raman band at 813 cm^{-1} denotes the RNA concentration within

the nucleus [44]. The cells in S phase are significantly active when
 compared to the quiescent cells from G0/1 phase (Fig. 2A). This
 means the level of transcription occurring within the nucleus is
 elevated during S phase when compared to G0/1 phase resulting
 in more of RNA accumulation. Accordingly, the Raman band at
 813 cm^{-1} is stronger in S phase when compared to G0/1 phase
 (Fig. 2C). However, the peak at 813 cm^{-1} is specifically and sig-
 nificantly weak in TPA-induced cells from S phase (Fig. 2C). This
 could be due to one or both of the following reasons: (1) A signif-
 icant population of cells in S phase would be supporting a lytic
 infection. At this stage, the cellular machinery is overwhelmed by
 active KSHV replication and virus-induced host transcription shut-
 off – both of which may eventually result in cell death. Of these,
 the KSHV-induced host transcription shutoff specifically results in
 host cell RNA degradation and thus a weak 813 cm^{-1} band [27,
 45] and (2) it is a reflection of a complicated set of events occur-
 ring within the cells during reactivation. The peak at 830 cm^{-1}
 represents tyrosine side chains and vibrations in the adenine,
 thymine 1, and thymine 2 sugars [46, 47]. Tyrosine is a unique
 amino acid that can be specifically phosphorylated by kinases cru-
 cial in the transduction of signals from within the nucleus to the
 outside and *vice versa*; whereas adenine and thymine are the com-
 ponents of DNA. This peak is specifically stronger only in TPA-
 induced cells from S phase when compared to cells from G0/1 and
 S phases. This makes sense as TPA induces not only cell prolifer-
 ation but also reactivation of virus infection. These results proved
 the point that Raman tweezers can distinguish between cells from
 G0/1, S and TPA-induced cells from S phase. In other words,
 Raman tweezers efficiently deciphered the fingerprints of cells
 (cells in S phase) that had the propensity to support KSHV reactiva-
 tion. However, this approach could not identify the fingerprints
 of the cells actually supporting reactivation because TPA induced
 reactivation of only 20–25% of cells in S phase (Fig. 4D and E).

In order to specifically delineate the Raman spectra of cells
 supporting KSHV reactivation, we followed a novel approach
 where cells were sorted based on the state of infection (latent *ver-*
sus lytic) by a flow cytometer and then analysed by the Raman
 tweezers. The state of infection was determined by the expression
 of the KSHV lytic protein (gB) on the cell surface. KSHV gB is
 expressed on the surface of cells supporting a lytic infection [29].
 In order to screen only cells that were supporting KSHV reactiva-
 tion, we incubated the cells in growth medium after sorting them
 through the flow cytometer. This additional step of incubation for
 4 hrs was done for two reasons: (i) eliminate any further effect of
 TPA and (ii) equilibrate cells from the effect of staining procedure.
 The cells supporting KSHV reactivation had a weaker band at
 813 cm^{-1} and a stronger band at 830 cm^{-1} when compared to
 cells that were supporting a latent KSHV infection (Fig. 5B). These
 data were comparable to what was observed for TPA-induced
 cells from S phase (Fig. 2C). The Raman bands at 785 cm^{-1} and
 1095 cm^{-1} for cells supporting KSHV reactivation were signifi-
 cantly weak when compared to cells that were supporting a latent
 infection (Fig. 5B). Apart from this, the Raman band at 1128 cm^{-1}
 was significantly strong in cells supporting KSHV reactivation when
 compared to cells supporting a latent infection (Fig. 5B). The 785,

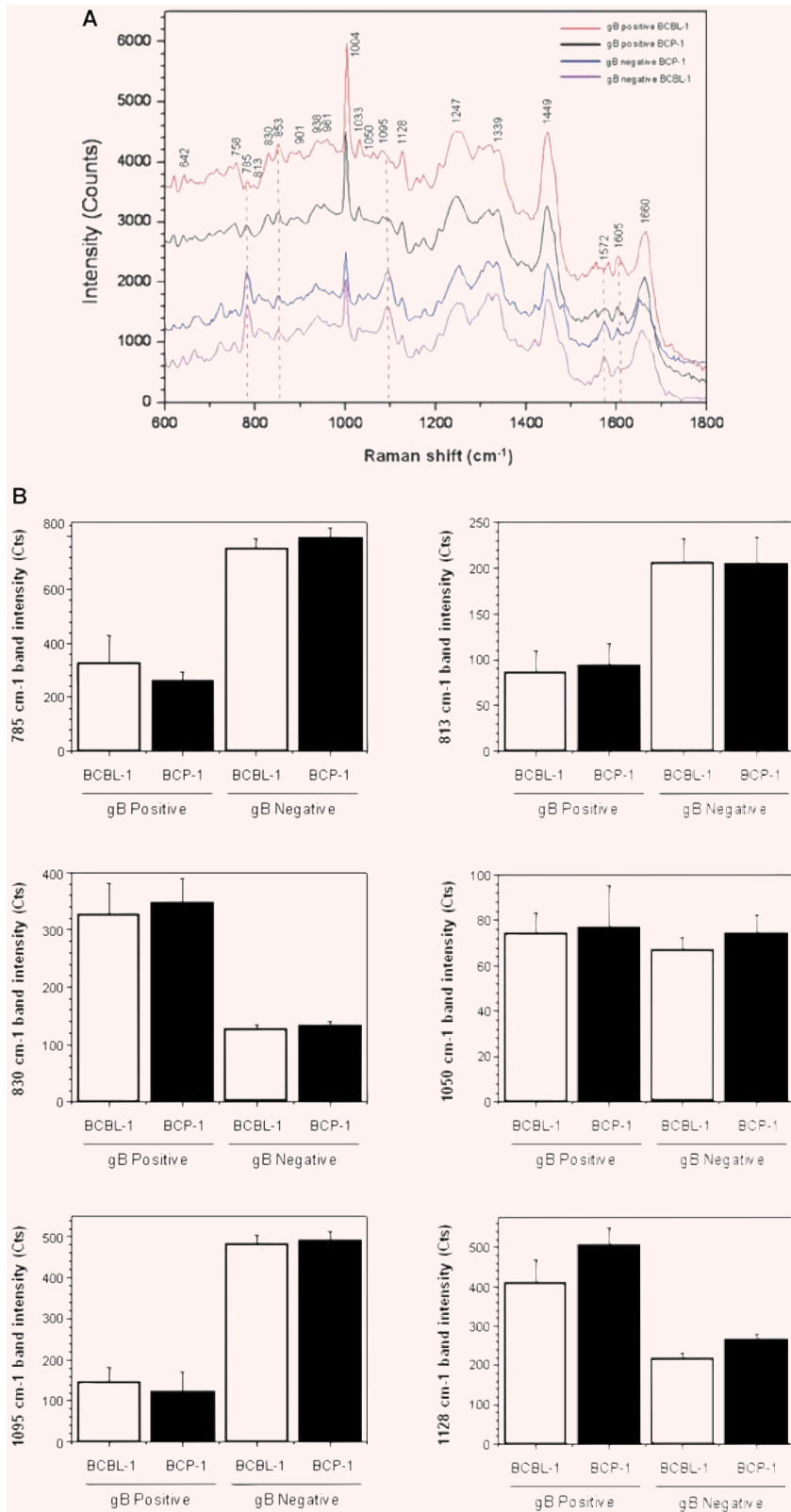


Fig. 5 Raman tweezers identifies the unique signature of cells supporting Kaposi's sarcoma-associated herpesvirus (KSHV) reactivation. **(A)** Average Raman spectra of individual BCBL-1 and BCP-1 cells that were actively supporting latent (gB negative) and lytic (reactivation; gB positive) KSHV infection in the fingerprint range from 600 to 1800 cm^{-1} is provided. Each spectrum was obtained by averaging the spectra of 20 individual cells. **(B)** Spectral changes in 785, 813, 830, 1050, 1095 and 1128 cm^{-1} Raman bands that occur between target cells supporting a latent and lytic KSHV infection is shown. The spectra are an average of data from 20 cells. Average values on columns with different superscripts are statistically significant ($P < 0.05$) by least significant difference.

Table 1 Raman bands that is unique for Kaposi's sarcoma-associated herpesvirus (KSHV) reactivation

Bands (cm ⁻¹)	Assigned function	References
785*	Phosphodiester bond C' ₅ -O-P-O-C' ₃ (DNA content); and pyrimidine nucleobases (U, T, C)	[49]
813*	RNA content	[44]
830*	Tyrosine side chains and vibrations in the adenine, thymine 1, and thymine 2 sugars	[45]
1095*	Phosphodioxy groups PO ₂ ⁻ of the DNA backbone (DNA content)	[47]
1128*	Vibrations of C-N in proteins and C-C in lipids	[48]
1050	Indicator of electronic structure of the nucleotides	[49]

Q10 *Denotes the five Raman bands that make up the fingerprint of cells supporting KSHV reactivation.

1095 and 1128 cm⁻¹ Raman bands indicate the phosphodiester bond C'₅-O-P-O-C'₃ and pyrimidine nucleobases; phosphodioxy groups PO₂⁻ of the DNA backbone; and vibrations of C-N in proteins and C-C in lipids, respectively [48–50].

To understand the physiological relevance of these peaks to KSHV reactivation, one has to understand the virus lytic infection. Like other herpesviruses, KSHV lytic infection is characterized by immediate shut off of the host RNA and DNA synthesis [51]. Herpesviruses are said to alter the host cell macromolecular metabolism in at least four manners: (i) host cell mRNA is degraded, (ii) transcription is shut off, (iii) cellular proteins are degraded and (iv) cellular proteins are redirected to perform function that directly benefit the lytic replication. All of the above cellular changes allow virus to replicate successfully, produce progeny virions, and finally kill the cells. These cellular changes are reflected

in the Raman bands (Table 1) in that the RNA (813 cm⁻¹) and DNA (785 and 1095 cm⁻¹) levels are lower in cells supporting KSHV reactivation. It feels as if the Raman band specific for DNA (1095 cm⁻¹) should have been stronger than what is observed based on the fact that the virus is actively replicating. These data on the peak 1095 cm⁻¹, we believe, are a strong reflection what is occurring within the infected cell during the late stages of lytic infection. Late stage of infection is classified based on the temporal expression of the KSHV encoded secondary late lytic gene (ORF 8 that encodes for gB, a structural protein). Genes involved in KSHV DNA replication are detected at significant levels during very early stages (by 14 to 20 hrs after lytic infection). They primarily aid in DNA repair and nucleotide metabolism. On the contrary, proteins and lipids that form part of KSHV (tegument, capsid and envelope-associated glycoproteins) are expressed very late during virus life cycle (about 34 hrs and later) [52]. This late spike in the viral proteins and lipids could be the result of strong Raman bands at 830 and 1128 cm⁻¹. All these five peaks seem to make up the distinct Raman fingerprints of the cells supporting KSHV reactivation.

Taken together, the results reported here describe the first use of a combination of molecular biology, biochemical assays and Raman tweezers in analysing the cellular events required to support a KSHV reactivation. This method will prove useful in the future to decipher the critical cellular events that trigger reactivation of KSHV latency. To date, all of the antivirals used to treat herpesvirus infections target only the lytic state of infection. Hence, these antivirals can never get rid of the virus completely. Understanding the molecular switch vital for the reactivation of latent infections will definitely open the door for developing new strategies capable of controlling, and perhaps eradicating, latent viral infections. We are certain that the present findings will serve as a model to unravel the mysteries surrounding virus latency.

Acknowledgements

This work was supported in part by NIH/NIBIB grant R21EB006483. We also thank Mr. Huxley for critically reading this manuscript.

References

1. **Chang Y, Cesarman E, Pessin MS, Lee F, Culpepper J, Knowles DM, Moore PS.** Identification of herpesvirus-like DNA sequences in AIDS-associated Kaposi's sarcoma. *Science*. 1994; 266: 1865–9.
2. **Hamden KE, Whitman AG, Ford PW, Shelton JG, McCubrey JA, Akula SM.** Raf and VEGF: emerging therapeutic targets in Kaposi's sarcoma-associated herpesvirus infection and angiogenesis in hematopoietic and nonhematopoietic tumors. *Leukemia*. 2005; 19: 18–26.
3. **Ganem D.** Human herpesvirus 8 and its role in the genesis of Kaposi's sarcoma. *Curr Clin Top Infect Dis*. 1998; 18: 237–51.
4. **Ensoli B, Sgadari C, Barillari G, Sirianni MC, Sturzl M, Monini P.** Biology of Kaposi's sarcoma. *Eur J Cancer*. 2001; 37: 1251–69.
5. **Grundhoff A, Ganem D.** Inefficient establishment of KSHV latency suggests an additional role for continued lytic replication in Kaposi sarcoma pathogenesis. *J Clin Invest*. 2004; 113: 124–36.
6. **Wang CY, Sugden B.** New viruses shake old paradigms. *J Clin Invest*. 2004; 113: 21–3.
7. **Dezube BJ, Zambela M, Sage DR, Wang JF, Fingerroth JD.** Characterization of Kaposi sarcoma-associated herpesvirus/human herpesvirus-8 infection of human vascular endothelial cells: early events. *Blood*. 2002; 100: 888–96.
8. **Blasig C, Zietz C, Haar B, Neipel F, Esser S, Brockmeyer NH, Tschachler E, Colombini S, Ensoli B, Sturzl M.**

- 1 Monocytes in Kaposi's sarcoma lesions are
2 productively infected by human her-
3 pesvirus 8. *J Virol.* 1997; 71: 7963–8.
- 4 9. **Diamond C, Brodie SJ, Krieger JN,**
5 **Huang ML, Koelle DM, Diem K, Muthui**
6 **D, Corey L.** Human herpesvirus 8 in the
7 prostate glands of men with Kaposi's sar-
8 coma. *J Virol.* 1998; 72: 6223–7.
- 9 10. **Staskus KA, Zhong W, Gebhard K,**
10 **Herndier B, Wang H, Renne R, Beneke J,**
11 **Pudney J, Anderson DJ, Ganem D, Haase**
12 **A.** Kaposi's sarcoma-associated herpesvirus
13 gene expression in endothelial (spindle)
14 tumor cells. *J Virol.* 1997; 71: 715–9.
- 15 11. **Whitby D, Howard MR, Tenant-Flowers**
16 **M, Brink NS, Copas A, Boshoff C,**
17 **Hatzioannou T, Suggett FE, Aldam DM,**
18 **Denton AS, et al.** Detection of Kaposi sar-
19 coma associated herpesvirus in peripheral
20 blood of HIV-infected individuals and pro-
21 gression to Kaposi's sarcoma. *Lancet.*
22 1995; 346: 799–802.
- 23 12. **Medveczky MM, Horvath E, Lund T,**
24 **Medveczky PG.** *In vitro* antiviral drug sen-
25 sitivity of the Kaposi's sarcoma-associated
26 herpesvirus. *Aids.* 1997; 11: 1327–32.
- 27 13. **Renne R, Zhong W, Herndier B, McGrath**
28 **M, Abbey N, Kedes D, Ganem D.** Lytic
29 growth of Kaposi's sarcoma-associated
30 herpesvirus (human herpesvirus 8) in cul-
31 ture. *Nat Med.* 1996; 2: 342–6.
- 32 14. **Jordan MC, Jordan GW, Stevens JG,**
33 **Miller G.** Latent herpesviruses of humans.
34 *Ann Intern Med.* 1984; 100: 866–80.
- 35 15. **Seiler P, Senn BM, Klenerman P, Kalinke**
36 **U, Hengartner H, Zinkernagel RM.**
37 Additive effect of neutralizing antibody and
38 antiviral drug treatment in preventing virus
39 escape and persistence. *J Virol.* 2000; 74:
40 5896–901.
- 41 16. **Duca KA, Shapiro M, Delgado-Eckert E,**
42 **Hadinoto V, Jarrar AS, Laubenbacher R,**
43 **Lee K, Luzuriaga K, Polys NF, Thorley-**
44 **Lawson DA.** A virtual look at Epstein-Barr
45 virus infection: biological interpretations.
46 *PLoS Pathog.* 2007; 3: 1388–400.
- 47 17. **Cook SD, Paveloff MJ, Doucet JJ,**
48 **Cottingham AJ, Sedarati F, Hill JM.**
49 Ocular herpes simplex virus reactivation in
50 mice latently infected with latency-associ-
51 ated transcript mutants. *Invest Ophthalmol*
52 *Vis Sci.* 1991; 32: 1558–61.
- 53 18. **Cesarman E.** The role of Kaposi's sar-
54 coma-associated herpesvirus (KSHV/HHV-8)
55 in lymphoproliferative diseases. *Recent*
Results Cancer Res. 2002; 159: 27–37.
- 56 19. **Glaser R, Kiecolt-Glaser JK, Speicher**
57 **CE, Holliday JE.** Stress, loneliness, and
58 changes in herpesvirus latency. *J Behav*
59 *Med.* 1985; 8: 249–60.
- 60 20. **Xie C, Mace J, Dinno MA, Li YQ, Tang W,**
61 **Newton RJ, Gemperline PJ.** Identification
62 of single bacterial cells in aqueous solution
63 using confocal laser tweezers Raman
64 spectroscopy. *Anal Chem.* 2005; 77:
65 4390–7.
- 66 21. **Lambert PJ, Whitman AG, Dyson OF,**
67 **Akula SM.** Raman spectroscopy: the gate-
68 way into tomorrow's virology. *Virology.*
69 2006; 3: 51.
- 70 22. **Akula SM, Ford PW, Whitman AG,**
71 **Hamden KE, Bryan BA, Cook PP,**
72 **McCubrey JA.** B-Raf-dependent expres-
73 sion of vascular endothelial growth factor-
74 A in Kaposi sarcoma-associated her-
75 pesvirus-infected human B cells. *Blood.*
76 2005; 105: 4516–22.
- 77 23. **Ramser K, Bjerneld EJ, Fant C, Kall M.**
78 Importance of substrate and photo-
79 induced effects in Raman spectroscopy of
80 single functional erythrocytes. *J Biomed*
81 *Opt.* 2003; 8: 173–8.
- 82 24. **Akula SM, Ford PW, Whitman AG,**
83 **Hamden KE, Shelton JG, McCubrey JA.**
84 Raf promotes human herpesvirus-8 (HHV-
85 8/KSHV) infection. *Oncogene.* 2004; 23:
86 5227–41.
- 87 25. **Medema RH, Herrera RE, Lam F,**
88 **Weinberg RA.** Growth suppression by
89 p16ink4 requires functional retinoblas-
90 toma protein. *Proc Natl Acad Sci USA.*
91 1995; 92: 6289–93.
- 92 26. **Dyson OF, Bryan BA, Lambert PJ, Ford**
93 **PW, Akula SM.** Beta1 integrins mediate
94 tubule formation induced by supernatants
95 derived from KSHV-infected cells.
96 *Intervirology.* 2007; 50: 245–53.
- 97 27. **Whitman AG, Dyson OF, Lambert PJ,**
98 **Oxendine TL, Ford PW, Akula SM.**
99 Changes occurring on the cell surface dur-
100 ing KSHV reactivation. *J Electron Microsc.*
101 2007; 56: 27–36.
- 102 28. **Bryan BA, Dyson OF, Akula SM.**
103 Identifying cellular genes crucial for the
104 reactivation of Kaposi's sarcoma-associat-
105 ed herpesvirus latency. *J Gen Virol.* 2006;
106 87: 519–29.
- 107 29. **Akula SM, Pramod NP, Wang FZ,**
108 **Chandran B.** Human herpesvirus 8 enve-
109 lope-associated glycoprotein B interacts
110 with heparan sulfate-like moieties.
111 *Virology.* 2001; 284: 235–49.
- 112 30. **McAllister SC, Hansen SG, Messaoudi I,**
113 **Nikolich-Zugich J, Moses AV.** Increased
114 efficiency of phorbol ester-induced lytic
115 reactivation of Kaposi's sarcoma-associat-
116 ed herpesvirus during S phase. *J Virol.*
117 2005; 79: 2626–30.
- 118 31. **Shaw AM, Braun L, Frew T, Hurley DJ,**
119 **Rowland RR, Chase CC.** A role for bovine
120 herpesvirus 1 (BHV-1) glycoprotein E (gE)
121 tyrosine phosphorylation in replication of
122 BHV-1 wild-type virus but not BHV-1 gE
123 deletion mutant virus. *Virology.* 2000;
124 268: 159–66.
- 125 32. **Hamden KE, Bryan BA, Ford PW, Xie C, Li**
126 **YQ, Akula SM.** Spectroscopic analysis of
127 Kaposi's sarcoma-associated herpesvirus
128 infected cells by Raman tweezers. *J Virol*
129 *Methods.* 2005; 129: 145–51.
- 130 33. **Lukas J, Agaard L, Strauss M, Bartek J.**
131 Oncogenic aberrations of p16INK4/CDKN2
132 and cyclin D1 cooperate to deregulate G1
133 control. *Cancer Res.* 1995; 55: 4818–23.
- 134 34. **Platt G, Carbone A, Mittnacht S.**
135 p16INK4a loss and sensitivity in KSHV
136 associated primary effusion lymphoma.
137 *Oncogene.* 2002; 21: 1823–31.
- 138 35. **Ford PW, Bryan BA, Dyson OF, Weidner DA,**
139 **Chintalgattu V, Akula SM.** Raf/MEK/ERK
140 signalling triggers reactivation of Kaposi's
141 sarcoma-associated herpesvirus latency. *J*
142 *Gen Virol.* 2006; 87: 1139–44.
- 143 36. **Krek W, DeCaprio JA.** Cell synchronization.
144 *Methods Enzymol.* 1995; 254: 114–24.
- 145 37. **Hinz M, Krappmann D, Eichten A, Heder**
146 **A, Scheidereit C, Strauss M.** NF-kappaB
147 function in growth control: regulation of
148 cyclin D1 expression and G0/G1-to-S-
149 phase transition. *Mol Cell Biol.* 1999;
150 19: 2690–8.
- 151 38. **Mao Y, Wu J, Skog S, Eriksson S, Zhao Y,**
152 **Zhou J, He Q.** Expression of cell proliferating
153 genes in patients with non-small cell lung
154 cancer by immunohistochemistry and cDNA
155 profiling. *Oncol Rep.* 2005; 13: 837–46.
- 156 39. **Ohrvik A, Lindh M, Einarsson R, Grassi J,**
157 **Eriksson S.** Sensitive nonradiometric
158 method for determining thymidine kinase
159 1 activity. *Clin Chem.* 2004; 50: 1597–606.
- 160 40. **Gross MK, Merrill GF.** Thymidine kinase
161 synthesis is repressed in nonreplicating
162 muscle cells by a translational mechanism
163 that does not affect the polysomal distribu-
164 tion of thymidine kinase mRNA. *Proc Natl*
165 *Acad Sci USA.* 1989; 86: 4987–91.
- 166 41. **Jess PR, Smith DD, Mazilu M, Dholakia**
167 **K, Riches AC, Herrington CS.** Early detec-
168 tion of cervical neoplasia by Raman spec-
169 troscopy. *Int J Cancer.* 2007; 121: 2723–8.
- 170 42. **Sun Y, Overman SA, Thomas GJ Jr.**
171 Impact of *in vitro* assembly defects on
172 *in vivo* function of the phage P22 portal.
173 *Virology.* 2007; 365: 336–45.
- 174 43. **Raso SW, Clark PL, Haase-Pettingell C,**
175 **King J, Thomas GJ Jr.** Distinct cysteine
176 sulfhydryl environments detected by
177 analysis of Raman S-hh markers of
178 Cys->Ser mutant proteins. *J Mol Biol.*
179 2001; 307: 899–911.

Q12

- 1
2
3
4
5
6
7
8
9
10
11
12
13
14
15
16
17
18
19
20
21
22
23
24
25
26
27
28
29
30
31
32
33
34
35
36
37
38
39
40
41
42
43
44
45
46
47
48
49
50
51
52
53
54
55
44. **Uzunbajakava N, Lenferink A, Kraan Y, Volokhina E, Vrensen G, Greve J, Otto C.** Nonresonant confocal Raman imaging of DNA and protein distribution in apoptotic cells. *Biophys J.* 2003; 84: 3968–81.
45. **Glaunsinger B, Ganem D.** Lytic KSHV infection inhibits host gene expression by accelerating global mRNA turnover. *Mol Cell.* 2004; 13: 713–23.
46. **Meng G, Chan JC, Rousseau D, Li-Chan EC.** Study of protein-lipid interactions at the bovine serum albumin/oil interface by Raman microspectroscopy. *J Agric Food Chem.* 2005; 53: 845–52.
47. **Dadarlat VM, Saxena VK.** Stability of triple-helical poly(dT)-poly(dA)-poly(dT) DNA with counterions. *Biophys J.* 1998; 75: 70–91.
48. **Borchman D, Tang D, Yappert MC.** Lipid composition, membrane structure relationships in lens and muscle sarcoplasmic reticulum membranes. *Biospectroscopy.* 1999; 5: 151–67.
49. **Notingher I, Verrier S, Haque S, Polak JM, Hench LL.** Spectroscopic study of human lung epithelial cells (A549) in culture: living cells *versus* dead cells. *Biopolymers.* 2003; 72: 230–40.
50. **Chan JW, Taylor DS, Zwerdling T, Lane SM, Ihara K, Huser T.** Micro-Raman spectroscopy detects individual neoplastic and normal hematopoietic cells. *Biophys J.* 2006; 90: 648–56.
51. **Chandriani S, Ganem D.** Host transcript accumulation during lytic KSHV infection reveals several classes of host responses. *PLoS ONE.* 2007; 2: e811.
52. **Jenner RG, Alba MM, Boshoff C, Kellam P.** Kaposi's sarcoma-associated herpesvirus latent and lytic gene expression as revealed by DNA arrays. *J Virol.* 2001; 75: 891–902.

Q13

Author Queries

- Q1 Author: Please check the rewording of the footnote.
- Q2 Author: An Exclusive Licence Form has not yet been received for this paper. Please go to: http://www.blackwellpublishing.com/pdf/JCMM_ETF.pdf and download and complete a form and return it to the Production Editor along with your corrections to the proofs. Note that we cannot publish your paper until the form is received.
- Q3 Author: Please check the edit in the sentence 'After 48 hrs...'.
- Q4 Author: Please check the inclusion of the manufacturer details in the sentence 'These blots were...'.
- Q5 Author: Please provide the detailed location of manufacturer 'Nikon' mentioned in the sentence 'Stained cells were...'.
- Q6 Author: Please provide the detailed location of manufacturer 'Nikon' mentioned in the sentence 'Stained cells were...'.
- Q7 Author: Please check the edit in the sentence 'After 36 hrs...'.
- Q8 Author: The first two colour figures will be published in colour free of charge. If you would like the additional figures in your article to be published in colour, please download and complete a colour work agreement form from http://www.blackwellpublishing.com/pdf/JCMM_CWA.pdf and return it to the Production Editor along with your proof corrections, at fax number +44 (0)131 226 3803.
- Q9 Author: Please provide the expansion of 'FAC' in the sentence 'The results from...'.
- Q10 Author: Please check the edits made in the 'References' column of the table.
- Q11 Author: Please provide the complete list of authors in reference 11.
- Q12 Author: Please provide the complete page range in reference 21.
- Q13 Author: Please provide the complete page range (if available) in reference 51.